Journal of Nuclear Materials 379 (2008) 24–32

Contents lists available at ScienceDirect

Journal of Nuclear Materials

journal homepage: www.elsevier.com/locate/jnucmat

On the tenuous nature of passivity and its role in the isolation of HLNW

Digby D. Macdonald *

Center for Electrochemical Science and Technology, Department of Materials Science and Engineering, Pennsylvania State University, 201 Steidle Bldg, University Park, PA 16802, USA

A B S T R A C T

The use of reactive metals and their alloys (e.g., Ni–Cr–Mo–W–Fe and Fe–Cr–Ni alloys) for isolating high level nuclear waste (HLNW) from the biosphere relies upon a continuing state of kinetic passivity of the metal surface. Without this state, which is due to the formation and continued existence of a 'passivating' oxide film, the alloy would react rapidly with components of the ambient environment (oxygen, water) and the structural integrity of the container would be compromised. The stability of the barrier oxide layers of bilayer passive films that form on metal and alloy surfaces, when in contact with oxidizing aqueous environments, is explored within the framework of the point defect model (PDM) using phase-space analysis (PSA), in which the rate of growth of the barrier layer into the metal, (dL^+/dt), and the barrier layer dissolution rate, (dL^-/dt), are plotted simultaneously against the barrier layer thickness, assuming that both processes are irreversible. A point of intersection of dL^-/dt with dL^+/dt indicates the existence of a metastable barrier layer with a steady state thickness that is greater than zero. If $dL^-/dt > (dL^+/dt)_{L=0}$, where the latter quantity is the barrier layer growth rate at zero barrier layer thickness, the barrier layer cannot exist, even as a metastable phase, as the resulting thickness would be negative. In any event, phase space analysis of the PDM permits specification of the conditions over which reactive metals will remain passive in contact with aqueous systems and hence of the conditions that must be met for the viable use of reactive metals and alloys for the isolation of HLNW.

1. Introduction

The conditions under which passive films exist on metal surfaces is a matter of great theoretical and practical interest, because the phenomenon of passivity is the enabler for our current, metals-based civilization [1]. Thus, our industrial systems and machines are fabricated primarily from the reactive metals and their alloys, including iron, nickel, chromium, aluminum, titanium, copper, zinc, zirconium, stainless steels, nickel-base alloys, and aluminum alloys, to name but a few. In one application of reactive metal alloys, nuclear power nations are currently developing strategies for isolating high level nuclear waste (HLNW) from the biosphere and most, if not all, of these strategies envision the use of canisters that are fabricated from reactive metals (e.g., Ni–Cr–Mo–W–Fe and Fe–Cr–Ni alloys). Consequently, the corrosion community is being asked to provide reasonable assurance to the public that isolation will be essentially complete for periods as long as one million years, which is two hundred times as far into the future that recorded human history is in the past. Never before in history has such a demand been made on a sector of the scientific community.

Although the phenomenon of 'passivity' has been known for about 170 years [2–4], and the conditions under which metals and alloys become passive have been systematically explored over the past 70 years [5–47], until recently no reasonably unifying theoretical treatment of the limits of passivity has emerged. While many theories and models for the passive state have been developed [5–48], most of the presently available models describe an already existing passive film and do not address the conditions under which the film may form or disappear. One of the few attempts to address this issue is that by Engell [29], who postulated that passive films can be thermodynamically stable or metastable, with film formation being governed by equilibrium thermodynamics in the first case and by the relative rates of formation and dissolution in the second. While Engell's work [29] made a valuable contribution to the theory of passivity, it did not resolve the theoretical issues with sufficient precision to allow specification of the exact conditions under which passivation/depassivation might occur (see below).

In this paper, the conditions under which passivity may occur and be lost are explored within the framework of the point defect model (PDM) [1] using phase-space analysis (PSA). It has been shown [31] that the PDM provides a comprehensive basis for describing the formation and destruction of passive films and hence allows specification of the conditions for the use of reactive metals in our metals-based civilization, in general, and for isolating HLNW, in particular [35,36]. For the purpose of illustrating the processes involved, a hypothetical 'Alloy X', having properties that are similar to the highly corrosion resistant Ni–Cr–Mo–W–Fe alloys (e.g., Alloy 22), is employed for the calculations. However, the

* Tel.: +1 814 863 7772; fax: +1 814 863 4718.
E-mail address: ddm2@psu.edu

0022-3115/$ - see front matter © 2008 Elsevier B.V. All rights reserved.
doi:10.1016/j.jnucmat.2008.06.004

author stresses that Alloy X does not represent any particular alloy currently in existence or use, because experiments underway to define the properties of the passive sate on Alloy 22, for example, are on-going. It is further assumed that the barrier oxide layer on the alloy is a defective chromic oxide ($Cr_{2+x}O_{3-y}$, x, $y > 0$), although the arguments are perfectly general and apply to any barrier layer.

2. Background

Passivity is normally manifest as a sharp drop in the anodic current density at a critical potential that is commonly referred to as the Flade potential (Fig. 1). For many metals and alloys, the current density drops by three or more orders in magnitude leading to a corrosion rate in the passive state that is lower than that in the active state (at the active peak just negative of the Flade potential) by the corresponding factor. Thus, a generally acceptable upper limit for the corrosion rate for components in industrial systems is 100 μm/year (0.01 mm/year); if that were increased by a factor of 1000 to 1 cm/year (10,000 μm/year), the use of metals in our metals-based civilization would be impractical. It is for this simple reason that passivity has been termed the 'enabler of our metals based civilization' [1]. For HLNW isolation containers, a corrosion rate of the order of 0.01 μm/year is required, corresponding to the loss of 1-cm of the container wall over a one million-year exposure.

At higher potentials, passivity is observed to break down on many metals and alloys and the dissolution rate of the substrate increases dramatically. This process is commonly due to the oxidative dissolution of the barrier layer ('oxidative depassivation' or 'transpassive dissolution' [35]); for example, in the case of chromium-containing alloys, which form chromic oxide barrier layers, the onset of transpassive dissolution is due to the reaction [31–35]

$$Cr_2O_3 + 5H_2O \rightarrow 2CrO_4^{2-} + 10H^+ + 6e^- \quad (1)$$

Note that this process results in the physical destruction of the film, such that the rate of dissolution, dL^-/dt, exceeds the rate of growth of the film at zero barrier layer thickness, $(dL^+/dt)_{L=0}$, (see later for nomenclature). Under these conditions, the barrier layer cannot exist under any circumstances (even in a metastable state, see below).

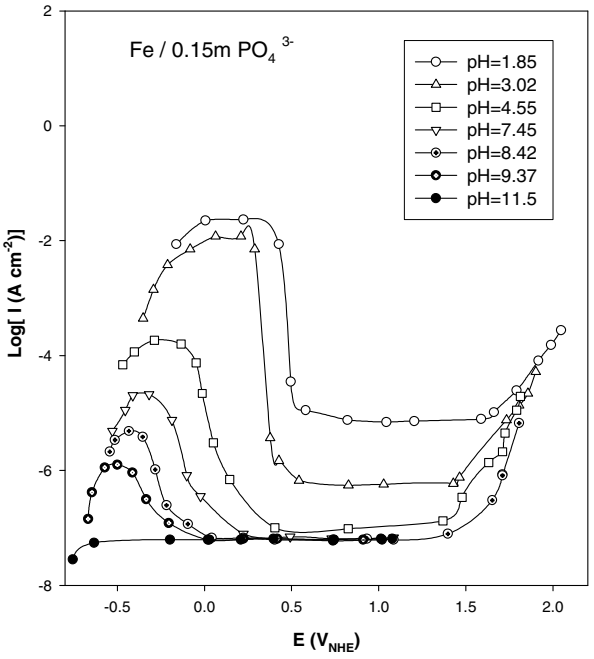

Fig. 1. Polarization curves for iron in phosphoric acid/sodium hydroxide buffer solutions at 25 °C as a function of pH (data taken from Sato [30]).

At lower potentials, dissolution occurs via the chemical process

$$Cr_2O_3 + 6H^+ \rightarrow 2Cr^{3+} + 3H_2O \quad (2)$$

which is not accelerated by increasing potential, because no change (increase) in the oxidation state occurs. The potential at which the dissolution rate of Cr_2O_3, due to Reactions (1), exceeds $(dL^+/dt)_{L=0}$ is known as the transpassive potential, E_{trans}, and previous work [34,35] shows that, at this potential, the barrier layer of the passive film is destroyed. However, before the transpassive potential is reached, the electronic characters of passive films on chromium-containing alloys frequently changes from n-type to p-type [37,38], corresponding to a change in the dominant defect in the barrier layer from the oxygen vacancy or metal interstitial to the cation vacancy. It is postulated in the PDM [1,35] that the cation vacancies are produced by the oxidative ejection of cations from the barrier layer into the solution/outer layer via the reaction

$$Cr_{Cr} + 4H_2O \rightarrow CrO_4^{2-} + V_{Cr}^{3'} + 8H^+ + 3e^- \quad (3)$$

which appears to become significant at potentials lower than E_{trans}, where the barrier layer lattice is not destroyed. Note that the Kroger–Vink notation is used in Eq. (3) to describe the various species in the system, with Cr_{Cr} and $V_{Cr}^{3'}$ indicating a Cr(III) cation in a normal site on the cation sub-lattice and a vacancy on the same sub-lattice, respectively, of the barrier layer. Reaction (3) leads to enhanced cation transmission through the barrier layer, and hence to a higher current density, while Reaction (1) results in a thinner barrier layer and also leads to a higher current [E_{trans}]. Of great significance is the fact that, in the case of both reactions, the oxidation state of the chromium cation in the film increases by three, so that the rates of the reactions are predicted to become highly potential-dependent, as observed. Transpassive dissolution is observed in a great number and of metal and metal alloy systems; the critical requirement appears to be that a sufficiently large increase occurs in the oxidation state of the principal cation within the barrier layer of the passive film (e.g., Cr_{Cr} in the Cr_2O_3 barrier layer on chromium-containing alloys) as the potential is increased in the positive direction [1].

A key question in this analysis concerns the nature of passivity of Alloy X in contact with oxidizing, aqueous environments. Embodied within this question is whether the passive film on the alloy is thermodynamically stable or meta-stable, and definition of the conditions under which a passive film cannot exist on the surface, even in the meta-stable state, thereby resulting in depassivation and hence in rapid corrosion. As noted above, the nature of passivity and depassivation is addressed in the present work within the framework of the Point Defect Model [1,31], which has been developed to describe, at the atomic scale, the growth and breakdown of passive films.

2.1. Point defect model (PDM)

The physico-electrochemical basis of the PDM is extensively discussed in the literature (Refs. 1 and 31 and citations therein), so that only a brief description will be given here.

The PDM postulates that passive films that form on metal and alloy surfaces in contact with oxidizing environments are bilayer structures comprising highly defective barrier layers that grow into the metal and outer layers that form via the hydrolysis of cations transmitted through the barrier layer and the subsequent precipitation of a hydroxide, oxyhydroxide, or oxide, depending upon the formation conditions, or by transformation of the outer surface of the barrier layer itself (an 'Ostwald ripening' process). In many systems (e.g., Ni and Cr), the barrier layer appears to be substantially responsible for the phenomenon of passivity. In other systems, such as the valve metals and their alloys (Al, Ta, Ti, Nb, Zr,) and iron (particularly at elevated temperatures), for example, the outer layer may form highly resistive coating that effectively separates

the reactive metal and the barrier layer from the corrosive environment. The 'sealing' of anodized aluminum is an example of how the outer layer may be manipulated $V_M^{\chi'}V_O^{\cdot\cdot}$ to achieve high corrosion resistance. In the present analysis, only the barrier layer is considered, because the passivity of chromium-containing alloys appears to be due to a thin barrier layer of defective Cr_2O_3 that forms on the surface in contact with the alloy. Thus, in these cases, the $M_i^{\chi+}$ barrier layer is clearly 'the last line of defense'.

The PDM further postulates that the point defects present in a barrier layer are, in general, cation vacancies ($V_M^{\chi'}$), oxygen vacancies ($V_O^{\cdot\cdot}$), and cation interstitials ($M_i^{\chi+}$), as designated by the Kroger–Vink notation (Fig. 2). Cation vacancies are electron acceptors, thereby doping the barrier layer p-type, whereas oxygen vacancies and metal interstitials are electron donors, resulting in n-type doping. Thus, on both pure metals and alloys, the barrier layer is essentially a highly doped, defect semi-conductor, as demonstrated by Mott–Schottky analysis [1], for example. Not unexpectedly, the situation with regard to alloys is somewhat more complicated than that for the pure metals. Thus, while the barrier layers on pure chromium and on Fe–Cr–Ni alloys (including the stainless steels) are commonly described as being 'defective Cr_2O_3', that on pure chromium is normally p-type in electronic character [37], while those on the stainless steels [37,38] are n-type. It is not known whether this difference is due to doping of the barrier layer by other alloying elements, or is due to the inhibition of cation vacancy generation relative to the generation of oxygen vacancies and metal interstitials, in the barrier layer on the alloys compared with that on pure chromium. The exact details are of little consequence for the following analysis and hence they will not be explored further in this paper.

As previously discussed, the defect structure of the barrier layer can be understood in terms of the set of defect generation and annihilation reactions occurring at the metal/barrier layer interface and at the barrier layer/outer layer (solution) interface, as depicted in Fig. 2 [1]. Regardless of the electronic type, that is, irrespective of the identity of the dominant defect in the system, Reactions (3) and (7), Fig. 2, are responsible for the growth and destruction of the barrier layer and any analysis of the stability of the layer must focus on these two reactions. That the barrier layer always contains oxygen vacancies is self-evident, since the rate of dissolution at the barrier layer/solution interface is always finite.

As noted elsewhere [1], the rate of change of the barrier layer thickness for a barrier layer that forms irreversibly on a metal or alloy surface can be expressed as $c_3 = -\alpha_3\chi\beta\gamma$

$$\frac{dL}{dt} = \Omega k_3^0 e^{a_3 V} e^{b_3 L} e^{c_3 pH} - \Omega k_7^0 (C_{H^+}/C_{H^+}^0)^n e^{a_7 V} e^{c_7 pH}, \tag{4}$$

where $a_3 = \alpha_3(1-\alpha)\chi\gamma$, $a_7 = \alpha_7\alpha(\Gamma-\chi)\gamma$, and $c_7 = \alpha_7\beta(\Gamma-\chi)\gamma$ (Table 1). In these expressions, Ω is the mole volume of the barrier layer per cation, ε is the electric field strength within the barrier layer (postulated to be a constant and independent of the applied voltage in the steady state, because of the buffering action of Esaki tunneling [1]), k_i^0 and α_i are the standard rate constant and transfer coefficient, respectively, for the appropriate reactions depicted in Fig. 2 [i.e., Reactions (3) and (7)], α is the polarizability of the barrier layer/solution (outer layer) interface, (i.e., the dependence of the voltage drop across the interface, $\varphi_{f/s}$, on the applied voltage, V), β is the dependence of $\varphi_{f/s}$ on pH (assumed to be linear), $\gamma = F/RT$, χ is the oxidation state of the cation in the barrier layer, Γ is the corresponding quantity for the cation in solution, C_{H^+} is the concentration of hydrogen ion, $C_{H^+}^0$ is the standard state concentration, and n is the kinetic order of the barrier layer dissolution reaction with respect to H^+. Note that the rate of the dissolution reaction is voltage dependent if $\Gamma \neq \chi$; for $\Gamma < \chi$ (e.g., reductive dissolution of Fe_3O_4 to form Fe^{2+}), the rate decreases with increasing voltage, whereas for $\Gamma > \chi$ (e.g., oxidative dissolution of Cr_2O_3 to form CrO_4^{2-}) the rate increases with increasing voltage. For $\Gamma = \chi$ (e.g., dissolution of Cr_2O_3 as Cr^{3+}), the rate of dissolution is voltage independent. The reader will identify the first and second terms on the right side of Eq. (4) with dL^+/dt and dL^-/dt, respectively. Expressions for the base rate constants, k, for the reactions identified in Fig. 2 are given elsewhere [31].

By setting the left side of Eq. (4) equal to zero, the steady state thickness of the barrier layer, L_{ss}, is readily derived as

$$L_{ss} = \left[\frac{1-\alpha}{\varepsilon} - \frac{\alpha\alpha_7}{\alpha_3\varepsilon}\left(\frac{\Gamma}{\chi-1}\right)\right]V + \left[\frac{2.303n}{\alpha_3\varepsilon\chi\gamma} - \frac{\alpha_7\beta}{\alpha_3\varepsilon}\left(\frac{\Gamma}{\chi}-1\right) - \frac{\beta}{\varepsilon}\right]pH + \frac{1}{\alpha_3\varepsilon\chi\gamma}ln\left(\frac{k_3^0}{k_7^0}\right) \tag{5}$$

which is identical to the previously published expressions [1]. For systems in the passive state, $\Gamma = \chi$, Eq. (4) reduces to the somewhat simpler form of

$$L_{ss} = \left[\frac{1-\alpha}{\varepsilon}\right]V + \left[\frac{2.303n}{\alpha_3\varepsilon\chi\gamma} - \frac{\beta}{\varepsilon}\right]pH + \frac{1}{\alpha_3\varepsilon\chi\gamma}\ln\left(\frac{k_3^0}{k_7^0}\right), \tag{6}$$

where the parameters are as previously defined. Note that in deriving these expressions, the convention has been adopted that, for the

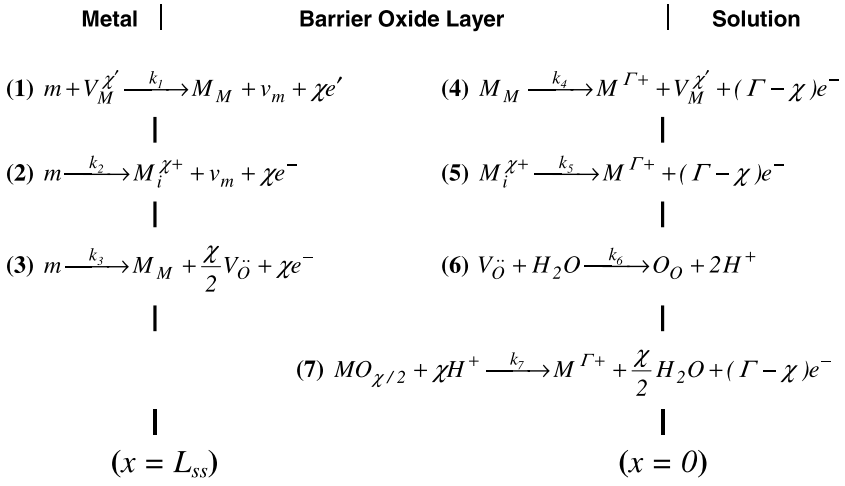

Fig. 2. Interfacial defect generation/annihilation reactions that are postulated to occur in the growth of anodic barrier oxide films according to the point defect model [1]. m = metal atom, $V_M^{\chi'}$ = cation vacancy on the metal sublattice of the barrier layer, $M_i^{\chi+}$ = interstitial cation, M_M = metal cation on the metal sublattice of the barrier layer, $V_O^{\cdot\cdot}$ = oxygen vacancy on the oxygen sublattice of the barrier layer, O_O = oxygen anion on the oxygen sublattice of the barrier layer, $M^{\Gamma+}$ = metal cation in solution.

rate of barrier layer dissolution, C_{H^+} and $C^0_{H^+}$ have units of mol/cm^3, but when used for defining pH, the units are the conventional mol/l. Thus, the standard states for the dissolution reaction [second term on the right side of Eq. (4)] and for the pH are 1.0 mol/cm^3 and 1.0 mol/l, respectively. The introduction of a standard state into the dissolution rate renders the units of k^0_7 independent of the kinetic order, n, without altering the numerical value of the rate.

The steady state passive current density is readily derived [1] as

$$I_{ss} = \Gamma F\left[k^0_2 e^{a_2 V} e^{b_2 L_{ss}} e^{c_2 pH} + k^0_4 e^{a_4 V} e^{c_4 pH} + k^0_7 e^{a_7 V} e^{c_7 pH} \cdot (C_{H^+}/C^0_{H^+})^n\right] \quad (7)$$

where the first, second, and third terms arise from the generation and transport of cation interstitials, cation vacancies, and oxygen vacancies, respectively, with the term due to the latter being expressed in terms of the rate of dissolution of the barrier layer [1]. This expression is derived, in part, by noting that the fluxes of a given defect at the two interfaces under steady state conditions are equal; in this way, the expression for the current can be formulated so as to avoid the defect concentrations at the interfaces.

3. Phase space analysis

Analysis of the stability of the barrier layer is best achieved by plotting Eq. (4) in 'phase space'; that is by plotting dL^+/dt and dL^-/dt versus L as a function of the applied voltage, pH, and other variables, as may be deemed appropriate [31], assuming that both the barrier layer formation and dissolution reactions are irreversible. For illustrative purposes, a schematic phase–space plot of Eq. (4) is shown in Fig. 3 for constant voltage and pH. This plot was prepared with the parameter values that are summarized in Table 1 [31].

As seen, the first term on the right side of Eq. (4) decreases exponentially with increasing L, provided that the reaction is considered to be irreversible, whereas the second term remains constant (does not depend on the barrier layer thickness, L). The point of intersection between dL^+/dt and dL^-/dt defines the steady-state film thickness, with $L_{ss} > 0$ being the only physically viable solution. Because a physically meaningful value of L_{ss} results from a balance between the rates of film growth and dissolution at the metal/film (m/f) and film/solution (f/s) interfaces, respectively, the film is only thermodynamically meta-stable. If $dL^-/dt \to 0$ then, from Fig. 3, $L_{ss} \to \infty$, corresponding to the thermodynamic equilibrium state.

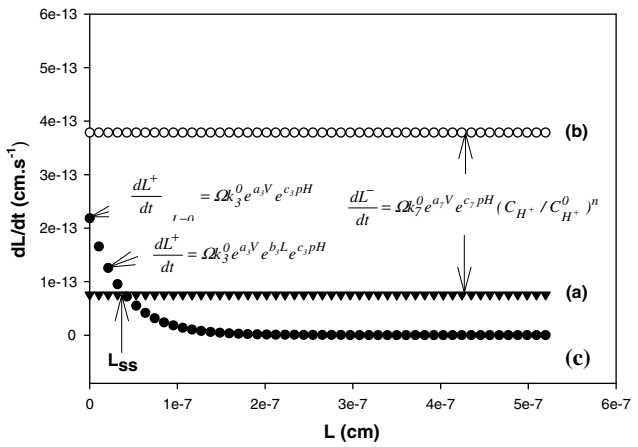

Fig. 3. Schematic of phase space analysis showing the steady state, passive condition (filled points, a and c) and the depassivated condition (filled and open circles, c and b). The intersection of (a) and (c) defines the steady state thickness of the metastable barrier layer. No intersection occurs between b and c for $L > 0$, so that a passive film cannot exist, even in the metastable state.

Table 1
PDM Parameter Values for Alloy X.[b]

Parameter	Value	Units	Identity/origin
Ω	14.59	cm^3/mol	Mol. volume per cation of the barrier layer (Calc. for Cr_2O_3 [a])
α	0.70		Polarizability of the barrier layer/solution
β	−0.005	V	Dependence of the potential drop at bl/sol interface on pH
α_1	0.15		Transfer coefficient for Reaction (1)
α_2	0.110		Transfer coefficient for Reaction (2)
α_3	0.120		Transfer coefficient for Reaction (3)
α_4	0.15		Transfer coefficient for Reaction (4)
α_5	0.15		Transfer coefficient for Reaction (5)
α_6	0.15		Transfer coefficient for Reaction (6)
α_7	0.50		Transfer coefficient for Reaction (7)
χ	3		Oxidation state of cation in barrier layer
Γ	3 or 6		Oxidation state of cation in solution
ε	2.00e−6	V/cm	Electric field strength
k^{00}_1	5.00e−06	s^{-1}	Base rate constant for Reaction (1)
k^{00}_2	1.00e−11	mol/cm^3 s	Base rate constant for Reaction (2)
k^{00}_3	5.00e−14	mol/cm^3 s	Base rate constant for film formation, Reaction (3)
k^{00}_4	1.00e−16	mol/cm^3 s	Base rate constant for Reaction (4)
k^{00}_5	1.00e−15	s^{-1}	Base rate constant for Reaction (5)
k^{00}_6	1.00e−25	mol/cm^3.s	Base rate constant for Reaction (6)
k^{00}_7	1.00e−13	mol/cm^3 s	Base rate constant for film dissolution, Reaction (7)
E_1–E_7	25.1	kJ/mol	Activation energy for Reactions (1)–(7)
T_0	353.15	K	Reference temperature
n	0.6		Kinetic order of film dissolution wrt [H$^+$]
$\phi^0_{f/s}$	−0.1	V	Constant

[a] Ω = Mol. Wt./density.
[b] In the original publication of this table [31], the negative signs in the exponents of the rate constants k^{00}_1 to k^{00}_7 were omitted in the final printing. Thus, k^{00}_1 should have read as above, not as 5.00e−06. An erratum was published [49].

Another way of looking at this issue is to note that, for a system at equilibrium, the net rates of all processes in the system must be zero; that is, for the passive film dL^+/dt and dL^-/dt are simultaneously zero. Clearly, this is only satisfied for dL^+/dt if $L_{ss} \to \infty$ and it is never satisfied by dL^-/dt for any real substance.

Accordingly, the equilibrium state is physically non-realizable, in contrast to the conclusion of Engell [29]. Furthermore, even if the composition of the solution is such that the outer surface of the barrier layer is at equilibrium, the barrier layer as a whole can not be at equilibrium, because of the transmission of cations as interstitials and via the cation vacancy structure. This is so, because the source of the cations (the metal) is thermodynamically less stable than is the barrier layer [this can be shown by adding Reactions (1), (4), (2), (5), (3), and (7)]. Of course, one could postulate that the system might come to equilibrium once the metal ion concentration in the solution had built up to the equilibrium value for the metal. However, if this occurred, the solution would be super saturated with respect to the barrier layer (and more so with respect to the outer layer) and precipitation would occur continuously until the metal was consumed.

Again, the passive film can not be in a state of equilibrium and the previously held notion that it is (or can be) must be abandoned.

It is evident from Fig. 3 that the physical condition that must be met for the barrier layer to exist on the surface is

$$\left(\frac{dL^+}{dt}\right)_{L=0} > \frac{dL^-}{dt} \quad (8)$$

This condition is equivalent to specifying that $L_{ss} > 0$. As is shown below, depassivation, particularly that due to transition to the transpassive state, is a catastrophic event that occurs over a minuscule change in an appropriate independent variable (potential or pH). Accordingly, for the purposes of defining the boundary

between the passivated and depassivated states, the inequalities may be replaced by equalities to read:

$$\left(\frac{dL^+}{dt}\right)_{L=0} = \frac{dL^-}{dt} \quad \text{or } L_{ss} = 0. \tag{9}$$

Eqs. (8) and (9) are, in a very literal sense, a statement of the conditions that must be met for the use of reactive metals in aqueous environments and hence the conditions that had to have been met for the development of our metals-based civilization.

In applying phase space analysis, the set of parameter values summarized in Table 1 are employed. These values are typical of those recently determined by Macdonald, et al. [42], for Alloy 22 in saturated NaCl brine and for iron in basic (NaOH) solutions [43], but the selected parameter values have been arbitrarily changed, so that the reader cannot take the values as being representative of those particular systems. This was done, because the studies in determining the parameter values are incomplete. Finally, the current treatment is valid only for acidic systems, where the dissolution rate is a positive function of $[H^+]$. Specifically, this requires that $pH \langle\langle pzc$, where pzc is the pH of zero charge for the oxide comprising the barrier layer. A more complete theory, one that covers the entire pH range, is currently being developed by the author.

3.1. Transition to the transpassive state

Phase space plots for Alloy X in acidified (pH 3), 6.256 m (sat.) NaCl at 50 °C are shown in Fig. 4. Two sets of plots are presented, linear–linear (a) and log-linear (b) plots, because of the difficulty of presenting the entire phenomenon on a single scale for the ordinate. As expected, the dissolution rate of the barrier layer, dL^-/dt, in the passive state, is potential-independent, whereas the film growth rate increases with increasing voltage for a constant barrier layer thickness [see Eq. (40) with $\chi = \Gamma$]. The values of $(dL^+/dt)_{L=0}$ are not shown in Fig. 4(a), because of the scale chosen for the ordinate, but they are evident in Fig. 4(b). As noted above, the point of intersection of dL^+/dt and dL^-/dt defines the steady state thickness, which is plotted as a function of voltage in Fig. 5. In the passive range, where $\Gamma = \chi = 3$, the barrier layer thickness varies linearly with voltage with a slope of $(1-\alpha)/\varepsilon = 1.5$ nm/V, which is typical of barrier layer growth. At $V = 0.9957 V_{SHE}$, the oxidation state of chromium, Γ, in the dissolution product increases to from 3 to 6 (chromate formation), and the thickness of the barrier layer is predicted to become zero. This sudden, catastrophic destruction of the barrier layer marks the transition of the system into the transpassive state [35,36].

The origin of the catastrophic destruction of the barrier layer is revealed in Fig. 6, in which the initial growth rate of the film at the

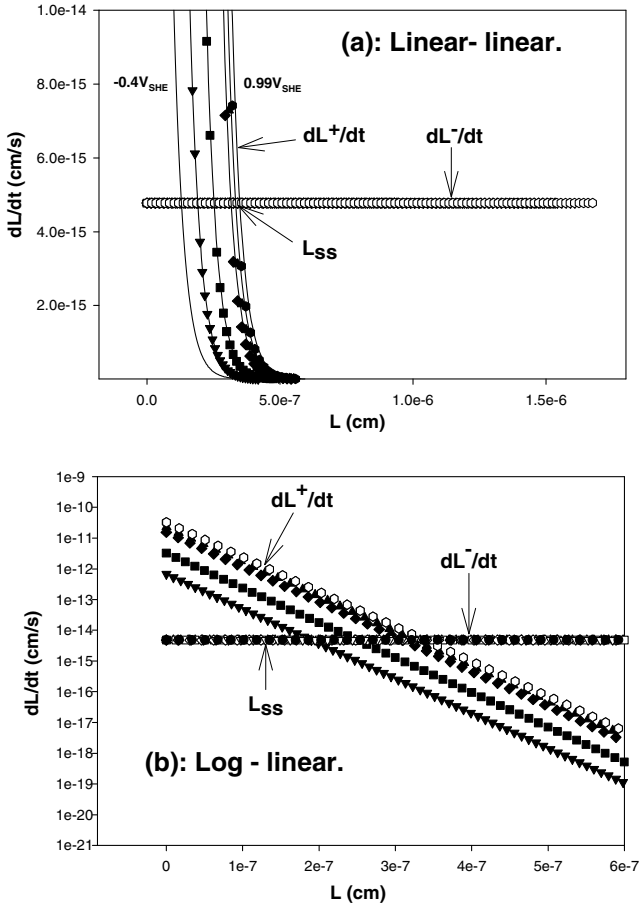

Fig. 4. Linear–linear (a) and log-linear (b) phase space plot for the barrier layer on Alloy X in acidified (pH 3), 6.256 m (sat.) NaCl at 50 °C, as a function of applied potential. The parameter values used in the calculation are given in Table 1. Note that an intersection occurs between dL^+/dt and dL^-/dt, so that a metastable barrier layer exists in all cases.

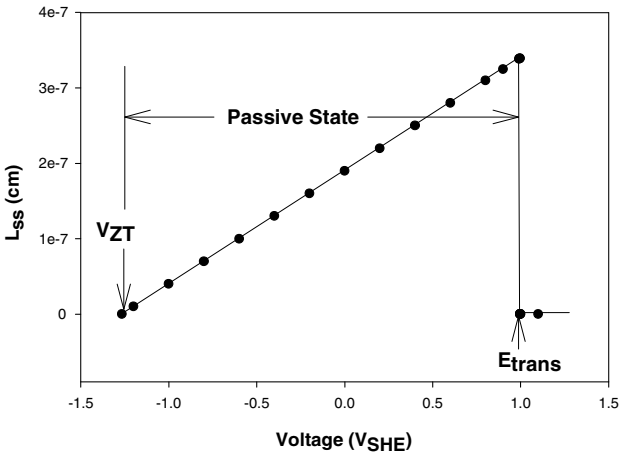

Fig. 5. Plot of the predicted steady state barrier layer thickness as a function of voltage. Loss of passivity is predicted to occur at 0.9957 V_{SHE} (E_{trans}), corresponding to the sudden reduction in the barrier layer thickness to zero at high potentials, due to the change in oxidation state of the cation in the film from χ to Γ, and at V_{ZT}, the potential at which the thickness of the barrier layer becomes zero at low potentials, due to the electrochemical reduction of the film.

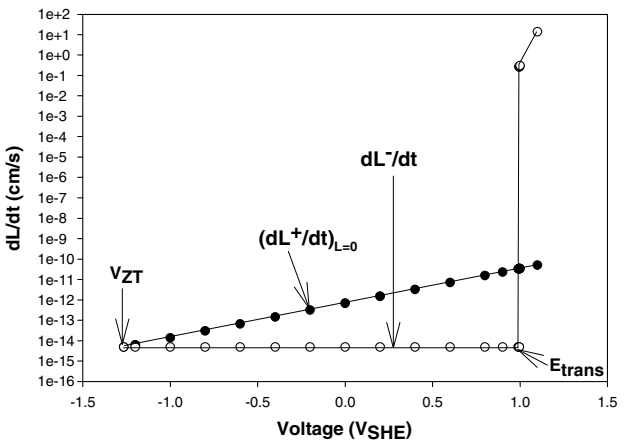

Fig. 6. Plots of the initial barrier layer growth rate and dissolution rate as a function of voltage for Alloy X in 6.256 m (sat.) NaCl at pH 3, 50 °C. Note that depassivation, corresponding to $dL^-/dt > (dL^+/dt)_{L=0}$ (transition into the transpassive state), occurs by the sudden increase in the barrier layer dissolution rate at E_{trans} (0.9957V_{SHE}).

metal/barrier layer interface, $(dL^+/dt)_{L=0}$, and the dissolution rate, dL^-/dt, are plotted against voltage. The initial barrier layer growth rate increases linearly with voltage through the critical transpassive potential, $E_{trans} = 0.9975V_{SHE}$, but the dissolution rate increases abruptly at E_{trans}, such that $dL^-/dt > (dL^+/dt)_{L=0}$. Thus, the transition into the transpassive state is induced by enhanced dissolution of the barrier layer at the barrier layer/solution interface, in a manner that leads to a catastrophic loss of the barrier layer.

Depassivation also occurs at very negative voltages, due to the barrier layer thickness extrapolating to zero. This may occur, because the film is electrochemically reduced to the metal, e.g., $Cr_2O_3 + 6H^+ + 6e^- \rightarrow 2Cr + 3H_2O$, or because it is reduced to a lower oxidation state species in the solution $[Cr_2O_3 + 6H^+ + 2e^- \rightarrow 2Cr^{2+} + 3H_2O]$. In this latter case, Γ is less than χ. At lower potentials, the system enters the passive-to-active transition. It is evident, then, that the passive state exists between these two extremes.

3.2. Acid depassivation

Log-linear phase space plots for Alloy X as a function of pH (not shown) predict that the barrier layer growth rate is only weakly dependent upon pH; this is primarily due to the small value of β. On the other hand, the dissolution rate of the barrier layer is a strong function of the concentration of H^+, by virtue of the value of the kinetic order, n. In any event, the thickness of the steady state barrier layer is predicted to decrease sharply with decreasing pH, such that at pH −1.2657, the barrier layer is destroyed. At this point, the surface has become depassivated and the substrate dissolves rapidly in the passive-to-active transition, depending upon the applied potential and the kinetics of the metal (active) dissolution reaction.

A more explicit demonstration of the fundamental cause of acid depassivation is shown in Fig. 7. In this figure, the initial film growth rate and the dissolution rate are plotted as a function of *pH*, demonstrating that the two functions intersect at pH −1.2657. Thus, for a lower pH < −1.237, $dL^-/dt > (dL^+/dt)_{L=0}$, and the barrier layer cannot exist on the surface, even as a metastable phase.

An important prediction of the PDM as elicited via phase space analysis, in comparison with the classical Pourbaix diagrams is that the passive state due to the existence of a defective chromic oxide film is predicted to persist to very low pH values (very highly acidic systems), whereas the purely equilibrium *E-pH* diagrams predict that the oxide should not be stable below about pH 3, depending upon the activity chosen for the dissolved metal cations. However, stainless steels are commonly used to store highly acidic solutions without displaying depassivation that would result in massive corrosion. This prediction is discussed further later in this paper in terms of kinetic stability diagrams (KSDs).

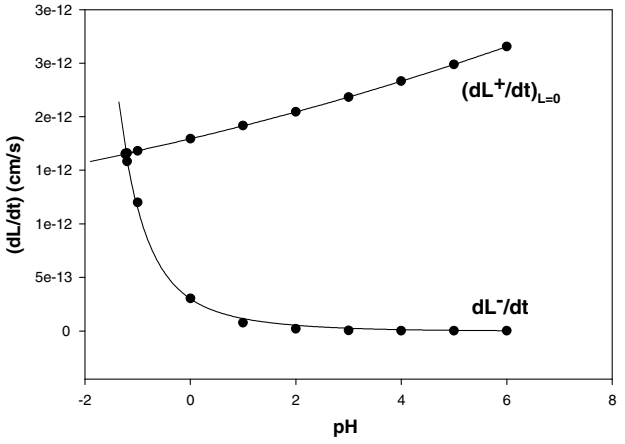

Fig. 7. Acid depassivation of Alloy X in 6.256 m (sat.) NaCl, $T = 50$ °C, $V = 0.300V_{SHE}$.

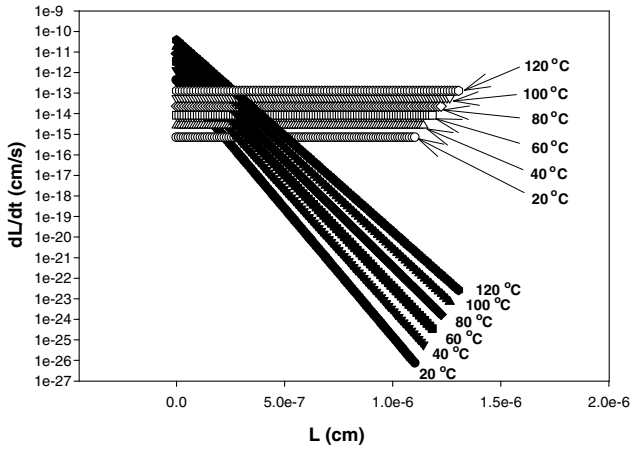

Fig. 8. Phase space plots for the barrier layer of the passive film on Alloy X in 6.256 m NaCl (sat.) at a potential of $0.300V_{she}$ and at a pH of 3.0 as a function temperature.

3.3. Effect of temperature

The predicted effect of temperature on the phase space plots for Alloy X in 6.256 m (sat.) NaCl at 50 °C and at a voltage of $0.300V_{SHE}$ is shown in Fig. 8. In this case, the ordinate data are plotted on the log scale, so that the phase space plots appear as linear relationships. As seen from Fig. 8, increasing temperature shifts both dL^-/dt and $(dL^+/dt)_{L=0}$ to higher values, in a manner that the steady state barrier layer thickness is predicted to be only weakly dependent on temperature. The shift is such that thermal depassivation is not predicted, at least for systems under the conditions that are predicted to exist in the Yucca Mountain repository (see Fig. 11, below).

4. Kinetic stability diagrams

The great contribution of Marcel Pourbaix in developing potential-pH ('Pourbaix') diagrams is firmly recognized in electrochemistry and corrosion science and these diagrams have proven to be powerful tools in analyzing physico-electrochemical phenomena in fields ranging from electrochemistry to geochemistry. However, the diagrams provide *equilibrium* thermodynamic descriptions of electrochemical systems, whereas, as demonstrated above, passivity is a kinetic phenomenon, with the very existence of the barrier layer depending upon a judicious relationship between the kinetics of formation of the film and the kinetics of dissolution, as embodied in Eq. (8). The limitation of Pourbaix diagrams in interpreting passivity is well illustrated by the resolution of Faraday's paradox [45,46], which showed that the passivity of iron observed by Faraday in concentrated nitric acid can only be accounted for by the formation of a *metastable* magnetite (Fe_3O_4) barrier layer covered by an outer layer of a precipitated Fe(III) hydroxide, oxyhydroxide, or oxide.

The conditions specified above have been used to develop 'kinetic stability diagrams (KSDs)' as alternatives to the classical Pourbaix diagrams, noting that KSDs are kinetic descriptions of the passive state and hence are not encumbered by the need for the system to be at electrochemical equilibrium; a condition that never exists in the passive state, as demonstrated earlier in this paper and elsewhere [31]. A primitive KSD for Alloy X under acidic conditions at 50 °C is shown in Fig. 9. The figure is divided into

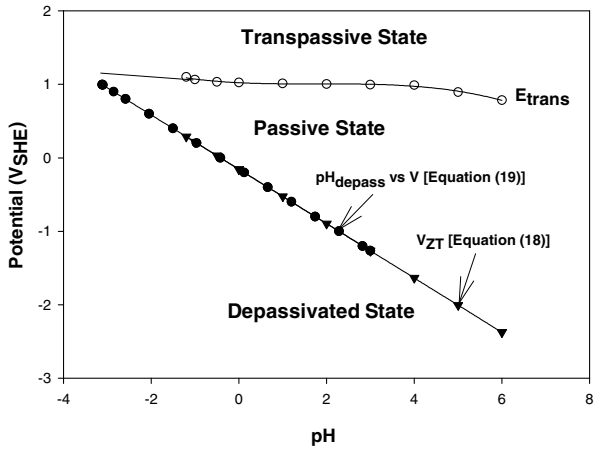

Fig. 9. Primitive kinetic stability diagram for Alloy X in acidic, 6.256 m NaCl at 50 °C. The passive state can exist only in the region indicated.

three regions; the transpassive state for potentials more positive than E_{trans}, the passive state at lower potentials, and the depassivated state at the most negative potentials and the most acidic systems. The boundary between the passive and depassivated states can be described by two equations, depending on whether *pH* or voltage is considered to be the independent variable, as described in Ref. [31].

Finally, the KSD indicates that Alloy X should be passive at very low pH values over a significant range of voltage, a prediction that is in keeping with observation for highly resistant stainless steels and Ni-Cr alloys, but which is not predicted by the classical Pourbaix diagrams.

5. Is depassivation likely?

Perhaps the most important question that might be asked in designing, and in specifying materials for, containers for a HLNW repository, in which the containers are in contact with an aqueous environment is: 'Will the containers remain passive over the design storage period?' Given that the design storage time may be very long (1 million years for the proposed repository at Yucca Mountain, Nevada), an experimental answer to this question is not feasible and we must rely upon theory, at least in part, to provide the necessary guidance.

In Fig. 10 is plotted temperature as a function of time for three storage scenarios at Yucca Mountain, according to the Lawrence

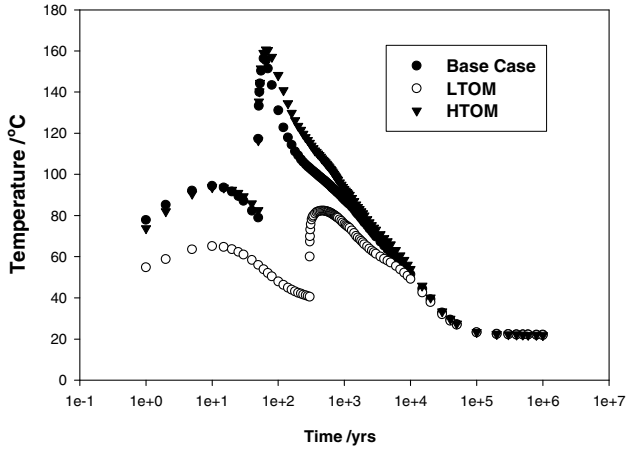

Fig. 10. Evolutionary paths with respect to temperature for the Yucca Mountain HLNW repository for the three scenarios defined by the LLNL.

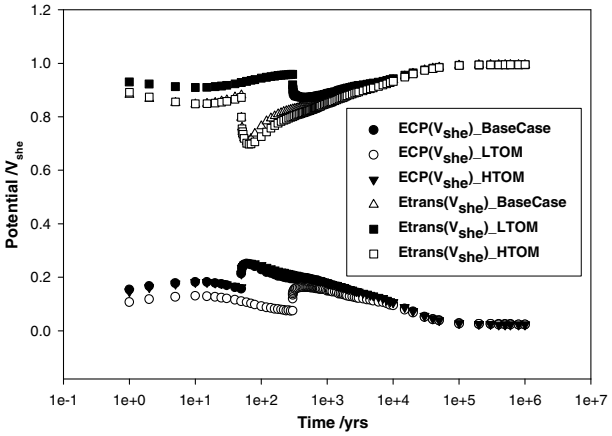

Fig. 11. Predicted evolutionary paths with respect to corrosion potential and transpassive dissolution potential over one million years for Alloy X in contact with saturated NaCl in the Yucca Mountain HLNW repository for the three scenarios defined by the LLNL.

Livermore Laboratory (see citation in Ref. [36]). (Note the logarithmic scale on the abscissa). The three scenarios differ by when the repository is closed; thus, the High Temperature Operating Mode (HTOM) will have closure occur soonest (approx. 50 years), while, for the Low Temperature Operating Mode (LTOM), closure is not envisioned to occur until about 300 years after the first placement of canisters in the drifts (tunnels). The base case (BC) is similar to the HTOM. The temperature initially increases as canisters are placed in the drifts, because of the heat generated by the decay of short-lived fission products. As these isotopes are depleted, the temperature then falls and continues to fall until the drifts are closed by backfilling. At that point (50 years for the HTOM and BC and about 300 years for the LTOM), the temperature is predicted to rise sharply, due to the loss of air convective cooling. The temperature is predicted to reach about 160 °C for the BC and HTOM and about 80 °C in the LTOM case. At longer times, the temperature is predicted to decay as the long-lived isotopes decay and to become more-or-less constant after about 100,000 years. In the LTOM, the temperature is sufficiently low that the container surface is expected to be wet over the whole storage period, but in the other two cases there will be a period shortly after closure where the surfaces are dry and 'wet' corrosion processes will not occur. This period is expected to last about 800 years. The temperature versus time traces shown in Fig. 10 essentially define the corrosion evolutionary paths for the three storage strategies.

In a previous study [36], the author used the Mixed Potential Model (MPM) to estimate the electrochemical corrosion potential of Alloy X over the three CEPs and the results are summarized in Fig. 11 (lower curves). Also plotted in this figure are the calculated oxidative depassivation potentials (transpassive potentials, upper curves). In making these calculations, it was assumed that the surface of the container was in continual contact with pH-neutral, saturated NaCl brine, which, in turn, was in contact with an ambient atmosphere containing 21% oxygen over the entire one million year storage period. The temperature was assumed to decay as shown in Fig. 10. It is evident that the calculated ECP does not approach the predicted transpassive potential over the entire CEP and hence there is no reason to believe that the environment could become sufficiently oxidizing to threaten the integrity of the passive film.

The situation with possible acid depassivation is somewhat more complex, since it would require a careful analysis of the solution phases that might develop on the container surface. However, it is possible to envision circumstances under which the hydrolysis

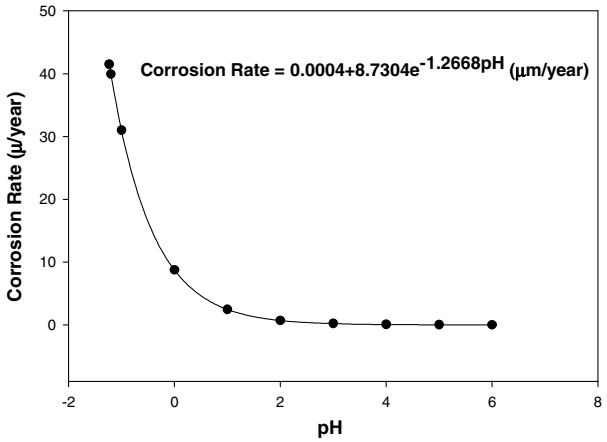

Fig. 12. Plot of calculated corrosion rate versus pH for Alloy X in contact with aerated, acidic, saturated NaCl (6.256 m) for the Yucca Mountain HLNW repository. $T = 50$ °C.

of metal cations may produce pH values as low as 2–3 [49]. This value is clearly not low enough to depassivate Alloy X, as predicted in this work, but it is possible that it might yield a corrosion rate of the passive alloy that would render the alloy impractical for fabricating HLNW isolation containers.

The corrosion rate of Alloy X was calculated as a function of pH from the MPM and PDM using the parameter values summarized in Table 1. The calculated corrosion rate is summarized in Fig. 12. As previously noted, the corrosion rate averages over the CEP would need to be below about 0.01 μm/year (1-cm per million years) in order that sufficient corrosion allowance be available to reasonably assure container integrity. Assuming the value of 0.01 μm/year for *CR* in the expression (see Fig. 12)

$$\mathrm{CR} = 0.0004 + 8.7304\mathrm{e}^{-1.2668\mathrm{pH}} \tag{10}$$

the pH value below which the pH should not be allowed to descend is found to be a modest 5.4. The reader is cautioned that this 'back-of-the-envelope' calculation refers to Alloy X and not to Alloy 22, because we do not yet have a complete set of values for the input parameters for the latter alloy for use in the PDM and the MPM for the full range of conditions that are of interest. From Faraday's law, the dissolution current density corresponding to a corrosion rate of 0.01 μm/year (3.17×10^{-14} cm/s) is about 1 nA/cm^2. Passive current densities of this magnitude for Alloy 22 in acidified brines (pH as low as 3) at 50 °C are indicated by the long term corrosion experiments of Lawrence Livermore National Laboratory [50] and of McMillion, et al. [51]. The parameter values presented in Table 1 yield a passive current density at 50 °C for Alloy X of 1 nA/cm^2 at pH 6, but at pH 3, the calculated value is about 100 nA/cm^2. This difference is immaterial in the present analysis, because the most important point of this work is that it provides a methodology for assessing the viability of any given alloy as a structural alloy for fabricating canisters, at least from a general corrosion viewpoint.

6. Summary and conclusions

The conditions under which reactive metals can exist within the passive state and hence may be used in our metals based civilization have been explored by phase space analysis (PSA) within the framework of the Point Defect Model (PDM). PSA demonstrates that a steady state in barrier layer thickness and passive current density exists only at the point of intersection of $\mathrm{d}L^+/\mathrm{d}t$ and $\mathrm{d}L^-/\mathrm{d}t$, where $\mathrm{d}L^+/\mathrm{d}t$ and $\mathrm{d}L^-/\mathrm{d}t$ are the rates of barrier layer growth at the metal/barrier layer interface and dissolution of the barrier layer at the barrier layer/solution interface, respectively, with the former being a decreasing exponential function of the barrier layer thickness. PSA also demonstrates that a passive film cannot exist in an equilibrium state and hence that the barrier layers of passive films on reactive metals and alloys in contact with oxidizing aqueous environments are meta stable in nature. Furthermore, PSA shows that, for a passive film (barrier layer) to exist on the metal surface, $(\mathrm{d}L^+/\mathrm{d}t)_{L=0} > \mathrm{d}L^-/\mathrm{d}t$. Violation of this condition occurs upon the transition of the system into the transpassive state, resulting in a sudden increase in the film dissolution rate brought about by an increase in the oxidation state of the dissolving species at the transition potential, E_{trans}. Alternatively, depassivation may occur due to a combination of a change in growth rate and/or film dissolution rate brought about by a causative agent in solution (H^+, as in the case of acid depassivation). In this latter case, no change in oxidation state is required. All of these depassivation phenomena can be described and predicted by a single equation, $L_{ss} = 0$ or equivalently $(\mathrm{d}L^+/\mathrm{d}t)_{L=0} = \mathrm{d}L^-/\mathrm{d}t$. Kinetic stability diagrams (KSDs), in which the regions of transpassive dissolution and depassivation are delineated from the passive state, are proposed as alternatives to the classical Pourbaix diagrams for describing the electrochemical states of passive metals and alloys in potential-pH space. Finally, the theory presented in this work is used to illustrate how the corrosion rate of an alloy can be calculated *ab initio* using values for various parameters in the point defect model that can be obtained by optimizing the PDM on electrochemical impedance spectroscopic (EIS) data.

Acknowledgments

The author gratefully acknowledges the support of this work by the US Department of Energy via Subcontract A20257JG1S from Innovation Design Technologies Inc., Henderson, Nevada.

References

[1] D.D. Macdonald, Pure Appl. Chem. 71 (1999) 951.
[2] H. Uhlig, Passivity of metals, in: R.P. Frankenthal, J. Kruger (Eds.), The Electrochemical Society, Dover, NJ, 1978, p. 1.
[3] C. Schönbein, Pogg. Ann. 37 (1836) 390. (reprinted in 196).
[4] M. Faraday, Experimental Researches, in Electricity, Vol. 2, Dover, NY, p. 234 (reprinted 1965).
[5] J.W. Schultze, M.M. Lohrengel, Electrochim. Acta 45 (2000) 2499.
[6] C.-O.A. Olsson, D. Landolt, Electrochim. Acta 48 (2003) 1093.
[7] International Symposium on Passivity, Schloss Heiligenberg, Germany; Z. Elektrochem., 62 (1958) 619.
[8] The Second International Symposium on Passivity, Toronto, Canada.; J. Electrochem. Soc. 110 (1963).; J. Electrochem. Soc. 111 (1964).
[9] The Third International Symposium on Passivity, Cambridge, UK, 1970.; Electrochim. Acta., 15 (1970).; Electrochim. Acta., 16 (1971).
[10] The Fourth International Symposium on Passivity, Airlie, VAR.P. Frankenthal, J. Kruger (Eds.), Passivity of Metals, The Electrochemical Society, Princeton, NJ, 1978.
[11] M. Froment (Ed.), The Fifth International Symposium on Passivity, Bombannes, France, 1983; Passivity of Metals and Semiconductors, Elsevier, Amsterdam, 1983.
[12] N. Sato, K. Hashimoto (Eds.), The Sixth International Symposium on Passivity, Sapporo, Japan, 1989, Passivity of Metals and Semiconductors, Pergamon Press, Oxford, UK, 1990.
[13] K. Heusler (Ed.), The Seventh International Symposium on Passivity, Passivation of Metals and Semiconductors, Clausthal, Germany, 1994, Special Issue of Mater. Sci. Forum., 185 (1995).
[14] M. B. Ives (Ed.), The Eighth International Symposium on Passivity of Metals and Semiconductors, Jasper, Alberta, Canada, May 9–14, 1999, The Electrochemical Society, 2001.
[15] A. Guntherschulze, H. Betz, Z. Phys. 68 (1931) 145.
[16] A. Guntherschulze, H. Betz, Z. Elekrochem. 37 (1931) 726.
[17] A. Guntherschulze, H. Betz, Z. Phys. 92 (1934) 367.
[18] E.J.W. Verwey, Physica 2 (1935) 1059.
[19] N. Cabrera, N.F. Mott, Rep. Progr. Phys. 12 (1948/1949) 163.
[20] F.P. Fehlner, N.F. Mott, Oxidat. Met. 2 (1970) 59.
[21] L. Young, Anodic Oxide Films, Academic Press, London, 1961.

[22] N. Sato, M. Cohen, J. Electrochem. Soc. 111 (1964) 512.
[23] K.J. Vetter, Electrochim. Acta 16 (1971) 1923.
[24] K.J. Vetter, F. Gorn, Electrochim. Acta 18 (1973) 321.
[25] R. Kirchheim, Electrochim. Acta 32 (1987) 1619.
[26] C.-Y. Chao, L.-F. Lin, D.D. Macdonald, J. Electrochem. Soc. 128 (1981) 1187.
[27] D.D. Macdonald, S.R. Biaggio, H. Song, J. Electrochem. Soc. 139 (1992) 170.
[28] K.E. Heusler, Corros. Sci. 31 (1990) 597.
[29] H.J. Engell, Electrochim. Acta 22 (1977) 987.
[30] N. Sato, Passivity of Metals, in: R.P. Frankenthal, J. Kruger (Eds.), The Electrochemical Society, Princeton, NJ, 1978, p. 29.
[31] D.D. Macdonald, J. Electrochem. Soc. 153 (2006) B213.
[32] C.-O.A. Olsson, D. Hamm, D. Landolt, J. Electrochem. Soc. 147 (2000) 4093.
[33] C.-O.A. Olsson, M.-G. Verge, D. Landolt, J. Electrochem. Soc. 151 (2004) B652.
[34] M.-G. Verge, C.-O.A. Olsson, D. Landolt, Corros. Sci. 46 (2004) 2583.
[35] D.D. Macdonald, Theory of the Transpassive State, H. H. Uhlig Award Lecture, The Electrochemical Society Spring Meeting, San Francisco, CA, May, 2001.
[36] D.D. Macdonald, The holy grail: deterministic prediction of corrosion damage thousands of years into the future, in: Proceedings of the International Workshop Pred. Long Term Corros. Behav. Nucl. Waste Systs. (Commissariat a l'Energie Atomique and Pennsylvania State University), Cadarache, France, Nov. 26–29 (2001). Euro. Fed. Corros. Publ. (Ed. D. Ferron and D. D. Macdonald), No. 36, p. 75 (2003).
[37] H. Tsuchiya, S. Fujimoto, O. Chihara, T. Shibata, Electrochim. Acta 47 (2002) 4357.
[38] C. Sunseri, S. Piazza, F. DiQuarto, J. Electrochem. Soc. 137 (1990) 2411.
[39] O. Pensado-Rodrguez, O.M. Urquidi-Macdonald, J.R. Flores, D.D. Macdonald, Bilayer film structure modeling for lithium dissolution in alkaline solutions, in: P.M. Natishan (Ed.), Passivity and Its Breakdown, Proc. Electrochem. Soc. 97-26 (1997) 870.
[40] O. Pensado-Rodriguez, J. Flores, M. Urquidi-Macdonald, D.D. Macdonald, J. Electrochem. Soc. 146 (1999) 1326.
[41] P. Park, M. Urquidi-Macdonald, D.D. Macdonald, ICONE (12th Int. Conf. Nucl. Eng., Nuclear Energy – Powering the Future), Hyatt Regency Crystal City, Arlington, VA, USA, April 25–29, 2004, Paper ICONE12-49098 (2004).
[42] D.D. Macdonald, A. Sun, N. Priyantha, P. Jayaweera, J. Electroanal. Chem. 572 (2004) 421.
[43] Jun Liu, Brian M. Marx, Digby D. Macdonald, Analysis of Electrochemical Impedance Data for Iron in Borate Buffer Solutions, in: P. Wang, T. Zachry (Eds.), Nuclear Waste Management: Accomplishments of the Environmental Management Science Program, ACS Symposium Series 943, American Chemical Society, Washington, 2006.
[44] E. Sikora, D.D. Macdonald, Electrochim. Acta 48 (2002) 69.
[45] T.S. de Gromoboy, L.L. Shreir, Electrochimica Acta 3 (1966) 895–904; L.L. Shreir, in: L.L. Shreir, R.A. Jarman, G.T. Burstein (Eds.), Corrosion, third ed., vol. 1, Butterworth-Heinemann, Oxford, 1994, p. 1.72.
[46] D.D. Macdonald, G.A. Cragnolino, Corrosion and erosion–corrosion of steam cycle materials, in: P. Cohen (Ed.), Water Technology for Thermal Power Systems, ASME, New York, New York, 1989. (Chapter 9).
[47] E. Sikora, J. Sikora, D.D. Macdonald, The point defect model vs. the high field model for describing the growth of passive films, in: K.R. Herbert, G.E. Thompson (Eds.), Proceedings of 7th International Symposium on Oxide Films on Metals and Alloys VII, vols. 94–25, 1994, p. 139.
[48] D.D. Eley, P.R. Wilkinson, Proc. Roy. Soc. (London) Ser. A 254 (1960) 327.
[49] D.D. Macdonald, J. Electrochem. Soc. 154 (2007) 12.
[50] J.H. Lee, K.G. Mon, D.E. Longsine, B.E. Bullard, A.M. Monilo, Mat. Res. Soc. Symp.-Proceedings 713 (2002) 61.
[51] L.G. McMillion, A. Sun, D.D. Macdonald, D.A. Jones, Met. Trans. A 36A (2005) 1129.